ACS OMEGA

http://pubs.acs.org/journal/acsodf
Article

Comparison of Transcription Elongation Rates of Three RNA Polymerases in Real Time

Priyanka Tare, Tuhin Bhowmick, Gurunath Katagi, Arnab China, and Valakunja Nagaraja*

Cite This: *ACS Omega* 2023, 8, 47510−47519
Read Online

ABSTRACT: RNA polymerases (RNAPs) across the bacterial kingdom have retained a conserved structure and function. In spite of the remarkable similarity of the enzyme in different bacteria, a wide variation is found in the promoter−polymerase interaction, transcription initiation, and termination. However, the transcription elongation was considered to be a monotonic process, although the rate of elongation could vary in different bacteria. Such variations in RNAP elongation rates could be important to fine-tune the transcription, which in turn would influence cellular metabolism and growth rates. Here, we describe a quantitative study to measure the transcription rates for the RNAPs from three bacteria, namely, *Mycobacterium tuberculosis*, *Mycobacterium smegmatis*, and *Escherichia coli*, which exhibit different growth kinetics. The RNA synthesis rates of the RNAPs were calculated from the real-time elongation kinetic profile using surface plasmon resonance through a computational flux flow model. The computational model revealed the modular process of elongation, with different rate profiles for the three RNAPs. Notably, the transcription elongation rates of these RNAPs followed the trend in the growth rates of these bacteria.

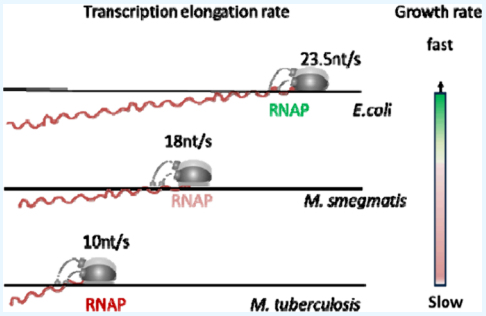

INTRODUCTION

Regulation in response to changing nutrient conditions is vital for free-living microbes, which must rapidly sense and respond to their environment to optimize fitness.[1] The variation in the growth of an organism is a cellular response to environmental factors. Nutrient availability, physical stress such as temperature and pH, presence of predators, and immunomodulatory molecules act as a cue for cells to alter their growth rates.[2] Modulation of growth by altering the rate of metabolism thus appears to be one of the mechanisms employed by microorganisms to combat the environmental stresses.[1] Within a single cell, the growth seems to affect the rate of metabolism and vice versa as the cell transits through exponential and stationary phases.[3]

RNA polymerase (RNAP), the central player in transcription, is remarkably well conserved in the bacterial kingdom. The mechanisms of transcription initiation, elongation, and termination also seem to be conserved across the species. However, the rates of NTP addition during transcription elongation could vary when RNAP encounters transcription pause sites.[4,5] The rates at which the RNAP transcribes along the DNA during the elongation could also vary in different species.[6,7] The elongation rate of transcription in *Escherichia coli* has been measured both *in vitro* and *in vivo* using many approaches.[4,7−11] In these experiments, depending on the conditions and techniques employed, the rates varied from 10 to 55 nt/s.[7,8,12−14] Thus, although there have been several studies to measure transcription elongation, no such studies using sensitive assays have been carried out in the genus *Mycobacterium*, which contains several important species including *Mycobacterium tuberculosis*. Here, we addressed the question whether transcription elongation rates of RNAPs could be correlated to the growth rates of different bacteria. Two species of mycobacteria with different growth characteristics were chosen along with the well-studied *E. coli* model system. *Mycobacterium smegmatis*, a fast-growing saprophytic bacterium, has a doubling time of 150−180 min, and *M. tuberculosis* has a doubling time of 18−24 h. These bacteria grow very slowly compared to *E. coli*, which has a doubling time of 18−20 min under laboratory conditions. Our quantitative elongation rate measurements reveal a pattern consistent with the growth characteristics of the three bacteria.

RESULTS

We measured the rates of the transcription elongation steps for the three RNAPs using SPR-based real-time monitoring (Figure 1). Biotinylated double-stranded DNA was used as a template in all of these real-time measurement experiments. The organization of the nontemplate strand of the DNA is shown in Supplementary Figure S1A. The DNA has a T7A1

Received: July 3, 2023
Accepted: September 11, 2023
Published: December 8, 2023

https://doi.org/10.1021/acsomega.3c04754
ACS Omega 2023, 8, 47510−47519

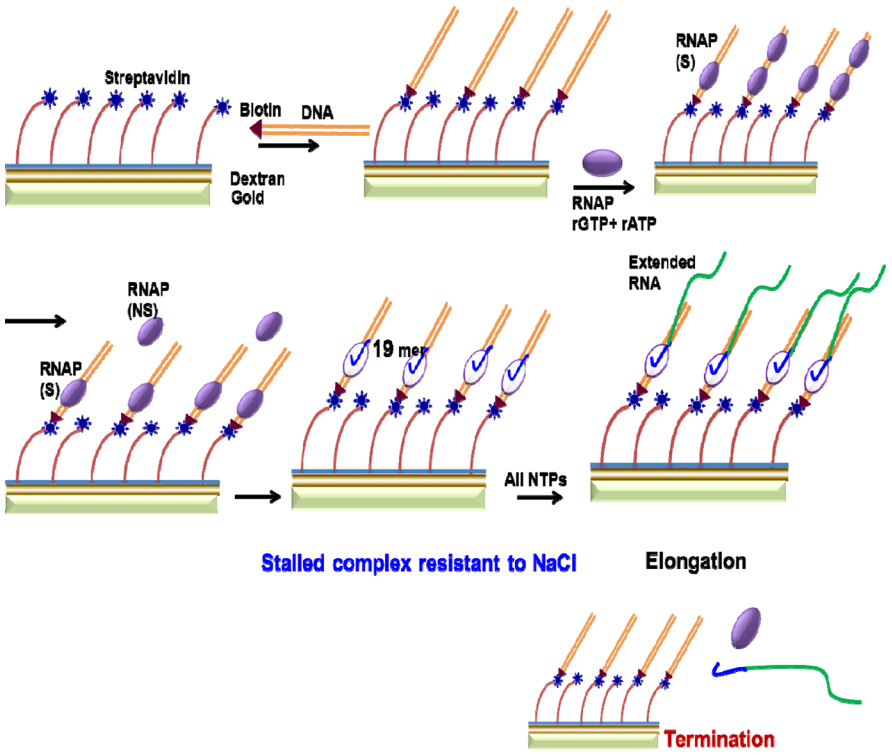

Figure 1. Schematic showing the steps carried out to monitor transcription initiation, elongation, and termination in real time.

promoter, a 19 nt long repeat of A+G, followed by a sequence either A+T rich ($T7A1_{50}$) (Figure 2A and Supplementary Figure S1B) or G+C rich ($T7A1_{62}$) (Supplementary Figure S1C). The T7A1 promoter was chosen to initiate the transcription for all the three RNAPs for the following reasons: (i) the promoter is well characterized in terms of the promoter−polymerase interaction and extensively used for studying transcription;[15,16] (ii) transcription elongation from the stalled elongation complexes (SECs) at the promoter has been standardized;[17] (iii) it is recognized and transcribed efficiently by *E. coli*, *M. smegmatis*, and *M. tuberculosis* RNAPs.[17−21] To measure the transcription elongation rates, we immobilized the biotinylated DNA. RNAP and a mixture of rGTP and rATP were added to the immobilized DNA to initiate the transcription and to synthesize a SEC with 19-mer RNA. After enriching the SEC on the chip by 250 mM NaCl wash (see Supplementary Figure S2), the elongation was resumed by chasing the complex with all the four ribonucleotides, and the rates of elongation were measured during this phase. The addition of all four rNTPs (rATP, rGTP, rCTP, and rUTP) to the stalled transcription elongation complex resulted in the increase in resonance units (RUs), indicating RNA synthesis. RNAPs were purified from *E. coli*, *M. smegmatis*, and *M. tuberculosis* (Supplementary Figure S3A). The sensorgram obtained for the three RNAPs is shown in Figure2B. This increase in RUs was converted to the equivalent units of NTP mass (1 RU = 4.58×10^{11} Da = 1.37×10^{9} nucleotides) in the RNA synthesized by the RNAP and retained on the SA chip.[22] The gain in NTP mass with respect to time was plotted to obtain the transcription elongation profile. Next, a simplistic model of transcription elongation was constructed using COmplex PAthway SImulator (COPASI) software, version 4.11.[23] The model addresses the RU increase due to the addition of nucleotide to the growing mRNA polymers and takes into account each elongation event to yield 120-mer transcripts (i.e., every event of elongation contributes to a mass equivalent of 101 nucleotides addition to the 19-mer SEC). This assumption is supported by the experimental analysis of elongation products, which shows the predominant population of 120-mer transcripts (Supplementary Figure S3B).

We observed that removing the immobilized transcription machinery from the streptavidin-coated surface reduced their efficiency for the second cycle of RNAP binding and subsequent RNA synthesis. To mitigate the problem, we added *M. tuberculosis* Rho to the transcription elongation complex having RNAP, DNA, and RNA. The subsequent increase in RUs suggested the binding of Rho. When NaCl was injected, the drop in RUs was seen. The RUs dropped below the level indicated for SEC, suggesting that Rho facilitated the release of RNA/RNAP from the transcription complex (Supplementary Figure S3C). The channels regenerated and thus could be reused for subsequent cycles of RNA synthesis.

Elongation Rates of *E. coli* RNAP and Its Mutant. First, we measured the elongation rates for *E. coli* RNAP (Figure 2A). To further ascertain, we measured the elongation rate for a mutant *E. coli* RNAP (Supplementary Figure S3A, Lane B8), characterized as an enzyme with a slower rate. *E. coli* B8 RNAP has a Q to P mutation at the 513th residue in the RpoB subunit that results in a slower rate of transcription.[14]

Minimal Kinetic Model for Transcript Elongation. TEC_{n-1} (transcription elongation complex) undergoes the addition of a nucleotide with a rate constant k_F, extending the nascent RNA polymer by 1 nt (TEC_n) and releasing PPi.[10] The reverse

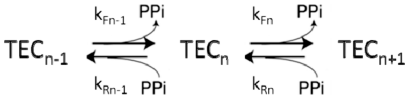

https://doi.org/10.1021/acsomega.3c04754
ACS Omega 2023, 8, 47510−47519

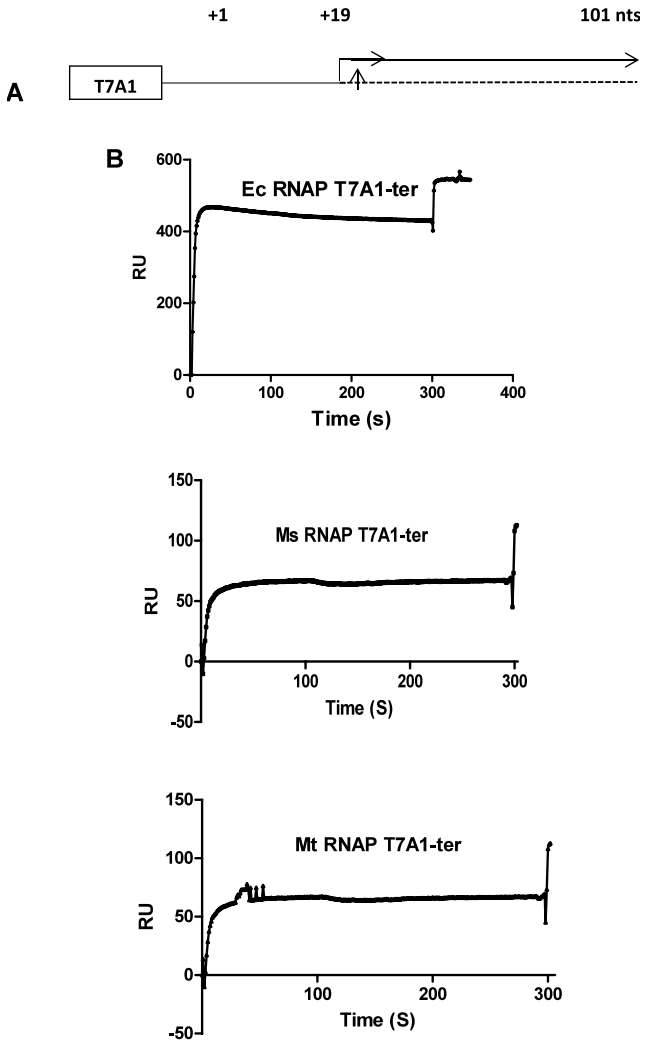

Figure 2. Elongation at T7A1$_{50}$-ter. (A) The DNA fragment used as the template is shown. The sequence transcribed for rate measurements had 50% G+C and was devoid of any terminator-like sequences (-ter). (B) The line plot showing the pattern of RU increase upon addition of NTP mix to the stabilized SEC on the (Strepta Avidin) SA chip is shown. The three plots were obtained using 200 nM Ec RNAP (*E. coli* RNAP), Ms RNAP (*M. smegmatis* RNAP), and Mt RNAP (*M. tuberculosis* RNAP) as indicated. The line plots were obtained by feeding the RU values corresponding to the RNA synthesis that were extracted from BIAevaluation software to GraphPad software, version 5.0.

reaction, pyrophosphorolysis, occurs with a rate constant k_R. For a simplistic representation of the process, the reversible translocation and NTP binding events that occur sequentially within each elongation were not explicitly included in the model. Based on the elongation kinetics, we built a kinetic model for the stepwise elongation of the TEC in COPASI using a set of differential equations, as shown below:

$$\frac{d[\mathrm{TEC}_i]}{dt} = \{k_{\mathrm{F}n-1}[\mathrm{TEC}_{n-1}] + k_{\mathrm{R}n}[\mathrm{TEC}_{n+1}]\} - \{k_{\mathrm{F}n}[\mathrm{TEC}_n] + k_{\mathrm{R}n-1}[\mathrm{TEC}_n]\} \quad (1)$$

where $19 < n < 120$ and n is an integer, TEC_n stands for transcription elongation complex at step n, and k_F and k_R are the rate constants for the forward and backward reactions, respectively.

The fitting of the model derived from COPASI to the experimental data is shown in Figure 3A,B (see Materials and Methods and Table S1 for details). Figure 3C depicts the profile of kinetic forward constant k_F vs elongation steps and the presence of different rate modules,[10,24] namely, initial, central, and terminal (see steps numbered as 20−26, 27−91, and 92−119 steps). The central module in Figure 3C represents a steady state of elongation addressed as the "monotonous mode" of transcriptional elongation with the forward rate constant k_{Fm} (for details, see Methods).

In our experimental setup, a k_{Fm} of 23.5 nt/s was calculated for the wild-type RNAP (Table 1 and Tables S1 and S3). Previous studies have determined the rates of *E. coli* RNAP within the range of 20 ± 7 nt/s.[4] Thus, our measurements are consistent with the earlier estimations, and the method also seems to be reliable. Determination of the transcriptional elongation rate for RNAP from the *E. coli* B8 strain (Figure 3B,C, Table 1, and Table S2) revealed a k_{Fm} of 17 nt/s, which is significantly slower than the wild-type RNAP (Figure 3C and Tables S2 and S3). These results thus essentially validate the method and the model employed to calculate the elongation rates.

Elongation Rates of Mycobacterial RNAPs. Next, we measured the transcription elongation rates of RNAPs from *M. smegmatis* and *M. tuberculosis* under the same set of experimental conditions and SPR measurements, as described above. These two related species show a large difference in the growth rates between themselves and *E. coli*. The SPR data from RNAPs (Figure 4A,B and Tables S4 and S5) from the two species of mycobacteria fitted to the COPASI model (Figure 4C and Table S6) revealed similar modular profiles for both the enzymes. The rates during the monotonous mode of transcription elongation were found to be 18.5 and 12 nt/s for *M. smegmatis* and *M. tuberculosis* RNAPs, respectively (Figure 4C and Table S6). These rates are substantially lower than that of *E. coli* RNAP. It is apparent that modular elongation rates follow the trend of growth rate, namely, *E. coli* > *M. smegmatis* > *M. tuberculosis*. Although the k_{Fm} values for the enzymes differ in these three species, the span of the monotonous mode remains almost the same (27−91 for *E. coli* RNAP and 30−93 for mycobacterial RNAPs). This observation can be attributed to RNA synthesis from the same promoter and a likely absence of any pause sequences in the DNA.

Effect of the DNA Sequence on the Elongation Rates. The template used for the above experiment contained DNA from pUC18 (sequence between 429 and 500 of plasmid) with an average G+C content of 50% (see Supplementary Figure S1). The elongation rates for the RNAP may change if the enzymes encounter a template whose G+C composition is higher than template 1. To address this point, the DNA sequence from *M. tuberculosis* gyrB (accession ID: CP009100.1) with a G+C content of 62% was chosen. This G+C sequence was inserted into the assay construct in place of the A+T-rich sequence used above (Supplementary Figure S4A). SPR experiments were carried out with *E. coli* and *M. smegmatis* RNAPs on this DNA. The data were fitted to the model (Tables S7 and S8 and Supplementary Figure S4B,C), which showed that the parameters for *M. smegmatis* RNAP did not change significantly with respect to the values derived from A+T-rich DNA (Supplementary Figure S4). The plots revealed that the plateau values (k_{Fm} = 18.5± nt/s) and the onset of the monotonous mode of elongation remained largely unaffected. In the case of *E. coli* RNAP, the onset of the monotonous

https://doi.org/10.1021/acsomega.3c04754
ACS Omega 2023, 8, 47510−47519

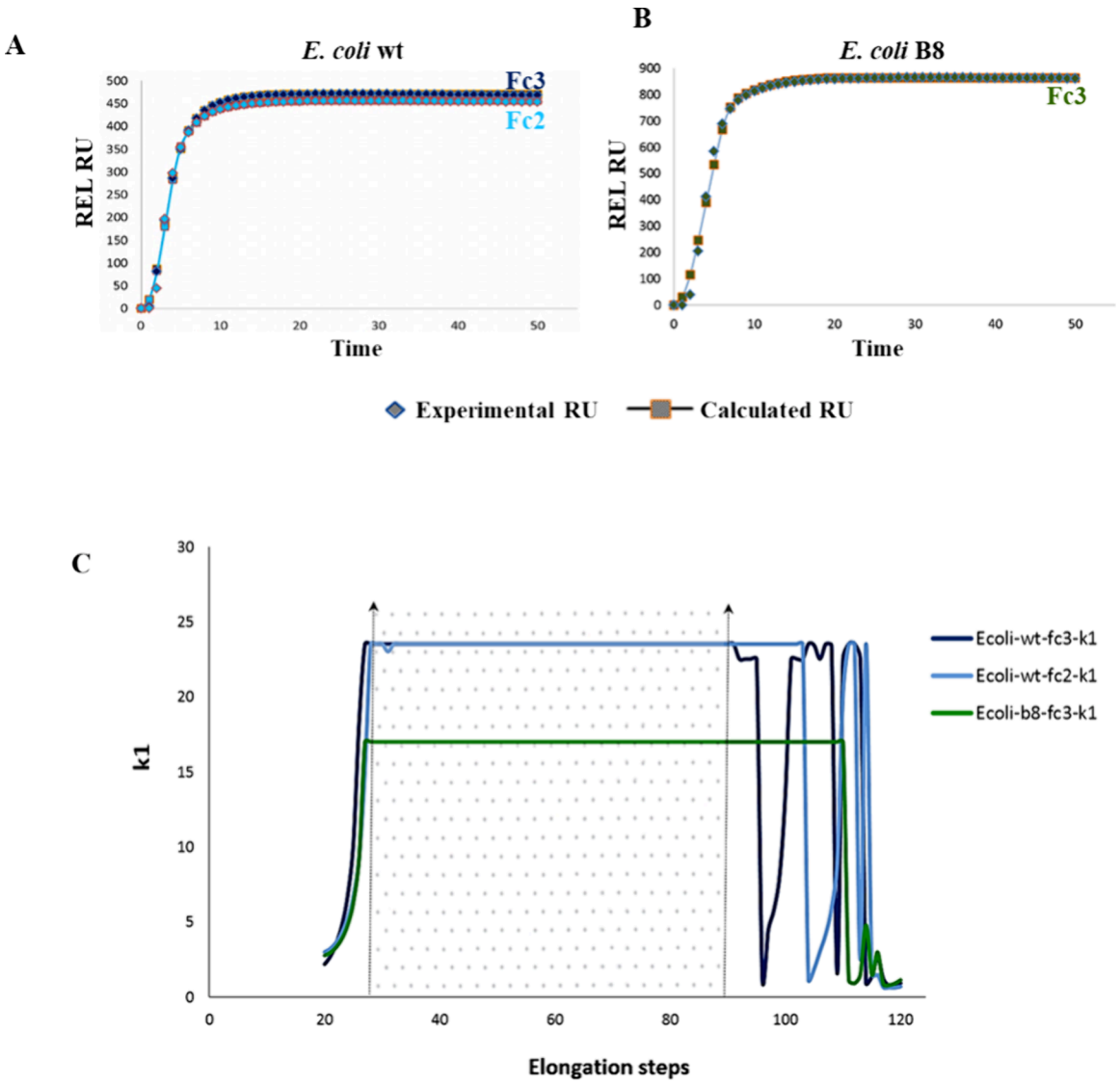

Figure 3. Elongation rates of *E. coli* WT and B8 RNAP. Determination of transcription elongation rates for *E. coli* WT and mutant B8 using SPR data. (A, B) Agreement of RU calculated from transcription elongation simulation (details in the text) with the experimental RU gain during the synthesis of 19-mer to 120-mer species, determined by SPR. The experimental and calculated data points are marked by colored diamond and rectangular boxes, respectively. Color coding is species specific and consistent through panels A and B. (C) Plot of forward kinetic constant $k1$ vs elongation steps depicting the presence of three rate modules, namely, initial 20 to 26, central 27 to 91, and terminal 92 to 119. The central module (steps 27 to 91, shaded) shows a steady rate of elongation, distinct for each species. The modular elongation rates appear to follow the trend of *E. coli* WT > *E. coli* B8. Fc, flow cell; the number indicates the flow cell data used for extraction. Each SPR chip contains four compartments known as flow cells (Fc1−4) of which Fc1 is used as the no DNA control. These Fc2−4 cells are used as distinct surfaces to immobilize the DNA and perform three replicates of the experiments. The data extracted from the sensorgrams and used for the calculation of $k1$ of each flow cell are indicated by the number.

Table 1. Span and the Forward Rate Constants for the Monotonous Mode (k_{Fm})

	domain boundary of the monotonous mode			
organism	experiment 1	experiment 2	experiment 1	experiment 2
E. coli (wild type)	(28−103)	(27−95)	23.5 (Fc2)	23.5 (Fc3)
E. coli (B8)		(27−110)		17 (Fc3)
M. smegmatis	(31−97)	(25−106)	18.5 (Fc3)	18.5 (Fc4)
M. tuberculosis	(23−92)	(25−94)	12 (Fc3)	12 (Fc4)

mode was shifted further down to the 39th step in comparison to the 27th step observed in the case of the A+T-rich DNA, although the k_{Fm} values were not significantly altered. The results suggest a lag in achieving the steady state for *E. coil* RNAP at G+C-rich DNA, while *M. smegmatis* RNAP had comparable profiles with both templates.

DISCUSSION

The mechanism of transcription has been extensively studied in *E. coli*, and the results have formed the basis to understand the process in many other bacteria. RNAP, the central molecular machine of transcription, is largely conserved across the bacterial kingdom. The mechanisms of transcription initiation, elongation, and termination are also very similar in different species. However, studies with the mycobacterial transcription machinery have revealed variations in the

https://doi.org/10.1021/acsomega.3c04754
ACS Omega 2023, 8, 47510−47519

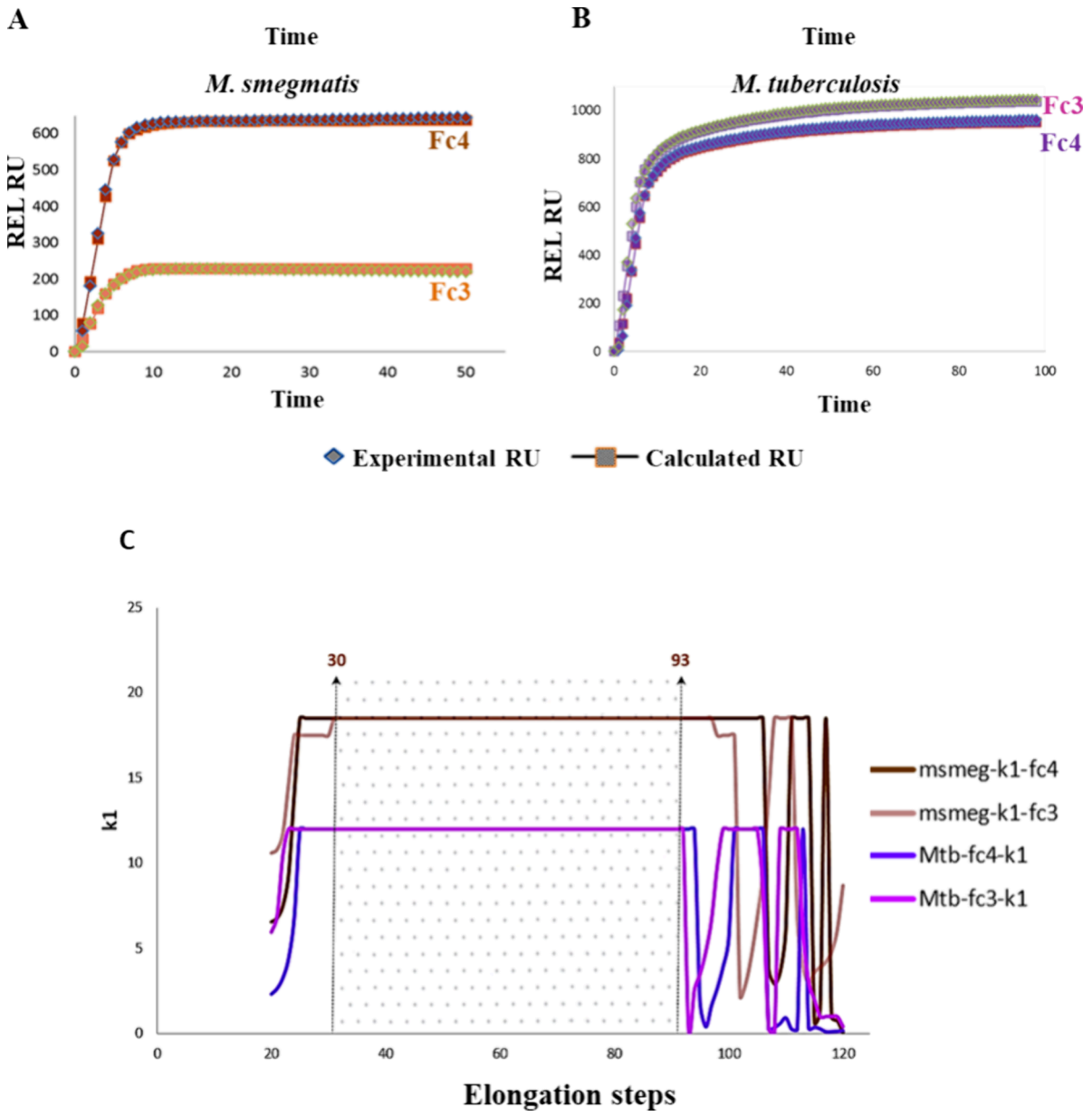

Figure 4. Determination of transcription elongation rates for *M. smegmatis* and *M. tuberculosis* using SPR data. (A, B) Agreement of RU calculated from transcription elongation simulation (details in the text) with the experimental RU gain during the synthesis of 19-mer to 120-mer species, determined by SPR. The experimental and calculated data points are marked by colored diamond and rectangular boxes, respectively. Color coding is species specific and consistent through panels A and B. (C) Plot of forward kinetic constant *k*1 vs elongation steps depicting the presence of three rate modules, namely, initial 20 to ∼30, central 31 to 93, and terminal 94 to 119. The central module (steps 27 to 91, shaded) shows a steady rate of elongation, distinct for each species. The modular elongation rates appear to follow the trend of *M. smegmatis* > *M. tuberculosis*. Fc, flow cell; the number identifies the flow cell data used for extraction (see the legend of Figure 3 for details).

transcription initiation patterns, distinct regulation of the key housekeeping promoters,[25,26] and novel aspects of intrinsic as well as factor-dependent transcription termination.[27−29] This study provides insights into the transcription elongation profile from the two well-studied species of mycobacteria.

The global kinetic model of elongation presented important information on the intrinsic behavior of the three RNAPs during transcription elongation. The RNAPs from three different species had different elongation rates. The analysis provided evidence to support the earlier suggestion that the transcription elongation is slower when an organism has a slower generation time.[7] Our data shows that the RNAP from the slowest-growing bacteria exhibits lowest elongation kinetics (Figure 4). Fittingly, the RNAP from the bacteria with an intermediate growth rate (*M. smegmatis*) had values higher than *M. tuberculosis* RNAP but lower than that of *E. coli* RNAP (Figures 3C and 4C). Notably, the *E. coli* B8 strain grew markedly slower than the wild type, consistent with our analysis.[30] The kinetic constants of the "monotonous mode" (k_{Fm}) during NTP addition is almost 2-fold greater for *E. coli* in comparison to that of *M. tuberculosis* (Table 1). The stepwise distribution of the elongation kinetics (Figures 3C and 4C) indicates that the transcript elongation processes of the organisms differ in terms of the rate constants and the span, namely, initial, monotonous, and terminal modules.

https://doi.org/10.1021/acsomega.3c04754
ACS Omega 2023, 8, 47510−47519

Earlier studies have shown that the mutations in RNAP affect the elongation rates.[14,31,32] One of these mutations (Q513P) in the β subunit of the enzyme in the *E. coli* B8 strain resulted in a holoenzyme with increased k_m for the NTPs, which was shown to impact the elongation rate.[14] The incorporation of radiolabeled nucleotides by both WT and B8 RNAPs was measured to calculate the elongation rates in this particular study. The elongation rates were found to be 16 and 4−5 nt/s for WT and B8 enzymes, respectively, when 0.4 mM rNTPs were used in the assays. However, at higher rNTP concentrations that mimic the physiological conditions, the rates of 23 and 11−12 nt/s were obtained for WT and B8 enzymes, respectively.[14] In our study described here using the SPR approach to measure the elongation rates, WT and B8 RNAPs using 1 mM rNTPs were 23.5 and 17 nt/s, respectively. In another study, which relied on single-molecule measurements, the average rates of 12.0 ± 2.1 and 3.4 ± 1.3 nt/s were obtained for the WT and B8 RNAPs, respectively.[8] Thus, although measurements by different approaches gave different values, invariably, the mutant polymerase had lower rates compared to the WT enzyme. The differences in the values between various studies for *E. coli* RNAP (see Table2)

Table 2. Rates of Elongation across a Diverse Set of Experiments

method	temperature	rate (nt/s)	organism	reference
optical trap single molecule	37 °C	12 ± 2.1	*E. coli*	8
microscopy single molecule	37 °C	12 ± 4+4.9	*E. coli*	13
microscopy single molecule	24 °C	20 ± 7	*E. coli*	4
optical trap single molecule	30 °C	16	*E. coli*	9
SPR bulk experiment	25 °C	10	*E. coli*	10
bulk transcription assays	37 °C	16	*E. coli*	14
Bulk transcription assays	37 °C	10	*M. tuberculosis*	6
in vivo (cells grown in LB media)[a]	37 °C	55[a]	*E. coli*	7
SPR bulk experiment	37°	23.5	*E. coli*	current study
		18.5	*M. smegmatis*	
		10	*M. tuberculosis*	

[a]LB, Luria-Bertani media.

have been attributed to the different techniques employed, nature of the template, concentrations of rNTPs, time duration of the assay, temperature, and methods of analysis. Moreover, the molecular heterogeneity of RNAP has been suggested to be a contributory factor in single-molecule measurements.[4,8,12] We suggest that mutations elsewhere in the enzyme other than Q513P RpoB could also affect elongation rates, given the crucial contribution of various subunits in the polymerase structure and functional organization. The B8 mutation that resulted in slower elongation rates of the *E. coli* RNAP is not found naturally in mycobacterial RNAPs,[14,33] thus ruling out its contributions for the intrinsic slower rates measured for these enzymes in this study. However, there are SNPs in these enzymes as the overall sequence identity between these enzymes is about 70%, which may account for the differences in the intrinsic rates observed with the enzymes studied in this work. Although the RNAP architecture and active centers are conserved across the eubacteria, the enzymes from various species show variations due to species-specific deletions, lineage-specific insertions, and single-nucleotide polymorphisms.[33−36] Thus, it would be a daunting task to identify individual residues responsible for the slower transcription elongation rate in RNAPs of different mycobacteria.

The sequence of DNA can also influence the kinetics of transcriptional elongation. Given that the overall G+C content in the genome of *E. coli* is lower than that of *M. smegmatis*, the effect may be related to the organism's intrinsic ability for its own DNA transactions. The stepwise distribution of the kinetic rates of elongation (Figures 3 and 4 and Supplementary Figure S4) in the model facilitates the correlation of the rates to the positional/sequence information on the DNA. The difference in the distribution of rates for RNAPs from *E. coli* and *M. smegmatis* in response to alteration in the DNA composition can be seen in the elongation plots (Supplementary Figures S1 and S4). In the $T7A1_{62}$ DNA, where the sequence after +19 position was 62% G+C for initial 50 nucleotides, the onset of the monotonous mode is delayed to the 39th nucleotide for *E. coli* RNAP. However, the *M. smegmatis* RNAP exhibited an elongation profile similar to the $T7A1_{50}$ DNA (Supplementary Figure S4D). The localized G+C-rich sites encountered in the genomes of the bacteria might cause some perturbations in *E. coli* RNAP during elongation but may not affect the overall monotonous mode of elongation. On the other hand, mycobacterial RNAP seems to prevail through the G+C sequence unaltered. Notably, the *in vivo* elongation rates will be influenced by various elongation factors that facilitate pause or relieve the pause. In a recent study, the trailing ribosome is shown to increase the speed of RNAP.[37]

From these results, it appears that the difference in the transcript elongation rates of *E. coli* and *M. tuberculosis* RNAP is not as much as the difference in their growth rates (μ), which differ by 44-fold (*M. tuberculosis* μ = 0.039 and *E. coli* μ = 1.730).[38−40] Thus, at first glance, the correlation between transcription elongation and growth rates seems to be less significant. However, when the data are extrapolated to the genome-wide scenario, a stronger correlation is apparent. Assuming that 30−50% genes would be transcriptionally active at a steady state during the exponential phase of the growth, the differences seen in one individual transcription unit measurement would be amplified when the whole-genome transcription is taken into consideration. Moreover, in many transcription units, repeated starts would also contribute to the differences. Further, unlike the *in vitro* experimental setup that takes into account only the minimal set of components required for transcription, the elongation rates *in vivo* would be influenced by a number of elongation factors. Moreover, the relative abundance of key machineries for the major processes would also contribute to the growth rate disparity. While *E. coli* genome has 7 rRNA operons and 4 initiator tRNA genes, *M. smegmatis* has only 2 rRNA operons and 1 initiator tRNA gene.[41−44] A single rRNA operon and an initiator tRNA gene are found in the *M. tuberculosis* genome.[42,44] Notably, the gene expression can be altered at the level of transcription initiation as observed for rRNA promoter transcription.[43−45] Transcription−translation coupling and the combinatorial and synergistic action of elongation factors further influence the *in vivo* elongation. The large difference in values seen in elongation rates with *E. coli in vitro* and *in vivo* measurements

https://doi.org/10.1021/acsomega.3c04754
ACS Omega 2023, 8, 47510−47519

could be attributed to some of these contributory factors. Thus, given that the transcription and translation are coupled,[46] the resultant accumulation of a smaller number of ribosomes[31] and other components of translation would also contribute to the slower growth rates for mycobacterial species.

METHODS

Buffers and enzymes used for modifying the DNA fragments were purchased from Roche. Biotinylated pUC primer, heparin, and deoxyribonucleotides were purchased from Sigma-Aldrich (Table 3). High-purity ribonucleotides, streptavidin assay (SA) chips, and surfactant P20 were procured from GE Amersham. RNAP from *E. coli*, *E. coli* B8, *M. smegmatis*, and *M. tuberculosis* were purified according to the protocols, as described previously.[48]

Table 3. Strains, Plasmids, and Oligonucleotides

plasmids	description	source
pUC18	a high copy *E. coli* plasmid used for DNA modifications and cloning	laboratory stock
pARN104	a pUC19-based plasmid modified in the laboratory	laboratory stock (49)

primers	sequence	source
biotinylated pUC forward	5′caggaaacagctatgac3′	Sigma
Pgyr Int reverse	5′gccgggcatggcgatagacgc3′	Sigma

bacteria	strains	description	source
E. coli	*MG1655*	*MG1655, rpoB*	laboratory stock
E. coli	*MG1655 B8*	MG1655, rpoB8 TetR, RifR	D. Jin, NIH (original sourced) and Sen, R, CDFD
M. smegmatis	*mc²115*	a high efficiency transformation strain of *M. smegmatis*	laboratory stock
M. tuberculosis	H37Ra	an attenuated strain of *M. tuberculosis* H37Rv	laboratory stock

Briefly, 4 L cultures of *E. coli* MG1655, *E. coli* MG1655 B8, *M. smegmatis* mc²155, and *M. tuberculosis* H37RA strains were grown until the midexponential phase. Cell pellets were resuspended in 40 mL of lysis buffer [50 mM Tris−HCl (pH 8.0), 2 mM EDTA, 5% glycerol, 230 mM NaCl, 5% glycerol, 0.1 mM DTT, 1 mM β-mercaptoethanol, 130 mg/mL lysozyme, and 23 mg/mL PMSF]. Cells lysed by sonication (*E. coli*) or French press (*M. smegmatis* and *M. tuberculosis*) were centrifuged at 50,000*g* for 1 h. TGED buffer [10 mM Tris−HCl (pH 7.9), 5% glycerol, 0.5 mM EDTA, and 0.1 mM DTT] was added, and the cell-free extracts were subjected to 0.35% PEI precipitation. The PEI pellet was homogenized with TGED buffer containing 400 mM NaCl. Extraction of proteins was carried out from the pellet using 50 mL of TGED containing 1 M NaCl, followed by 0−50% ammonium sulfate precipitation. The pellet was resuspended in 3 mL of TGED with 150 mM NaCl and loaded on a Superdex S-200 gel filtration column (bed volume 120 mL). The fractions enriched with RNAP were then pooled and loaded onto a heparin-Sepharose column (GE Healthcare) and eluted using a salt gradient of 150−800 mM NaCl in 1× TGED buffer. The purified proteins were loaded onto 8% SDS-PAGE and visualized using 0.1% Coomassie blue R-250 staining.

DNA Constructs. The $T7A1_{50}$ DNA fragment (300 bp) used for the transcription assays comprised T7A1 promoter sequence followed by 120 bp long 50% G+C-rich DNA for transcription.[17] The DNA fragment was cloned in pUC18 and was amplified using a biotinylated pUC forward primer and a vector-specific reverse primer for immobilization on the SA chip. The $T7A1_{62}$ DNA fragment was generated by ligating the fragment from the *gyrB* gene (amplified from pARN104)[47] that was 62% G+C rich. The fragment from the *gyrB* gene was cleaved using HinFI (NEB) and was ligated to the fragment containing T7A1 downstream to the +19 position and amplified using the biotinylated pUC forward primer and Gyr reverse primer (Table 3).

Monitoring the Transcription by SPR. The streptavidin (SA)-coated surface in the sensor chip was prepared for the injection as per the manufacturer's instructions (GE Amersham). Biotinylated DNAs were immobilized on the SA chips (flow rate of 5 μL/min). The rise in RUs was around 1400−1600. To reduce the mass transport effect, a low concentration of DNA (1.3 ng/μL) was used. The binding and elongation studies were carried out at 37 °C and at a flow rate of 10 μL/min, unless otherwise stated. The composition of running buffer was 20 mM Hepes (pH 7.8), 10 mM potassium chloride, 5 mM magnesium acetate, and 0.05% surfactant P20.[10] The RNAPs from *E. coli*, *M. smegmatis*, and *M. tuberculosis* were diluted in the 1× running buffer to a concentration of 100 or 200 nM, and a volume of 100 μL was used for the injections. rATP and rGTP were added along with the RNAP at a concentration of 1 mM across the control and sample cells at a flow rate of 10 μL/min. Buffer was passed at a flow rate of 10 μL/min for 20 min, followed by the injection of 250 mM NaCl. The chip was thoroughly washed for 10 min with running buffer at a flow rate of 50 μL/min. The NTPs (NTP mix) at a concentration of 1 mM (diluted in the running buffer) were added at a flow rate of 10 μL/min for 5 min.

***In Vitro* Transcription.** *In vitro* transcription reactions were carried out in standard transcription buffer (50 mM Tris−HCl (pH 8.0 at 25 °C), 3 mM magnesium acetate, 100 μM EDTA, 100 μM DTT, 30 mM KCl, 50 μg/mL BSA, and 5% glycerol). The DNA templates (10 ng) bearing the T7 promoter were incubated similarly as described for SPR experiments. *E. coli*, *M. smegmatis*, and *M. tuberculosis* RNAP (200 nM) was added in respective reactions, and the reactions were incubated for 10 min at 37 °C, followed by the addition of 100 μM rATP, rGTP, and rCTP and 10 μM nonradioactive rUTP and 1 μCi αP^{30} UTP. After 15 min of incubation, the reactions were terminated by the addition of stop buffer (95% formamide, 0.025% (w/v) bromophenol blue, 0.025% (w/v) xylene cyanol, 5 mM EDTA, 0.025% SDS, and 8 M urea) and heat inactivation at 90 °C for 5 min. The reactions were snap-cooled on ice for 5 min and resolved on 10% urea-PAGE.

Data Analysis. *Model Description.* The experimental observations were treated as a mass flux event, where a population of transcriptional units immobilized on the SPR probe add nucleotides to the growing chain of the mRNA polymer. Therefore, the mass of the transcriptional elongation product (in terms of the rNTPs added) at a moment "*t*" can be expressed as

$$\mathrm{TEC}_{i,t} = \sum_{i=19}^{i=120} (i - 19)[\mathrm{TEC}_i]_t \quad (2)$$

Steps of elongation from 19 mer to 120 mer based on the above relationships were treated as a set of 203 elements (1, initial number of 19 rNTPs; 101, k_F values; and 101, k_R values) that follow the relationships of eqs 1 and 2 using COPASI. Given the rate of pyrophosphorolysis to be minimal,[10] the

https://doi.org/10.1021/acsomega.3c04754
ACS Omega 2023, 8, 47510−47519

contribution of k_R was set to be 10^{-5}. Therefore, the major contributing parameters to the model are 102 (1, initial number of 19 rNMPs; 101, k_F values for 101 steps). The experimental observation that is addressed through the computational model starts at the point where all the transcriptional units are stalled at the 19-mer state. Based on the assumption that the initial 19-mer species have reached the 120-mer products upon completion, the initial number of 19 mers (n) can be calculated as $n = [\Delta RU \times 1.37 \times 10^9/(120 - 19)]$. This treatment also leaves the calculated elongation rate constants uninfluenced by the different numbers of SEC formation due to the minimal variations in transcription initiation. Thus, the calculated values reflect the intrinsic properties of the RNAPs from different organisms.

First, the values from the sensorgram were extracted using BIAevaluation software, version 3.0. The *E. coli* WT SPR data was used for fitting and model optimization. There are two sets of observations reported for *E. coli*, *M. tuberculosis*, and *M. smegmatis*. The RNAP slow mutant (B8) data were used to validate the global kinetic model. For *E. coli* and *M. smegmatis* RNAPs, additional experiments were carried out using DNA with higher G+C. Each experimental data set was fitted to the global model and was solved for the previously defined 102 independent variables. The fitting of the experimental data was done using COPASI. The initial solution was parameter optimized using successive cycles of differential evolution (2000 cycles) and particle swarm optimization (5000 cycles) protocols in COPASI. The refined model was plotted with experimental data. The attached supplementary tables contain all these solved data sets. The net profiles are reported in the main MS, in Figures 3 and 4 and Supplementary Figure S4. Among these large volumes of kinetic parameters, one important parameter is k_{Fm}, the forward rate constant of a steady kinetic module, referred to as the "monotonous mode". This module also has the fastest rate of elongation. The rate of nucleotide formation resulting in mass addition to the system can be expressed as

$$\tan\theta \propto k_{Fm}(n-1)[TEC_{28}]_t \quad (3)$$

where n is the number of steps within the monotonous mode and TEC_{28} is the particle number of the first species formed within the monotonous mode (for *E. coli*). The k_{Fm} for the monotonous mode of the transcription elongation process is 23.5 nt/s for *E. coli* WT. The above equation therefore explains that tan θ, the rate of rNTP addition, is a tangent to the RU vs time plot. Next, the experimental RU vs time plots for *M. smegmatis*, *E. coli* B8, and *M. tuberculosis* RNAP were fitted in COPASI following a similar process of *E. coli* WT RNAP.

■ ASSOCIATED CONTENT

Supporting Information

The Supporting Information is available free of charge at https://pubs.acs.org/doi/10.1021/acsomega.3c04754.

(Supplementary Text) Immobilization of DNA on the SA chips (PDF)

(Supplementary Figure S1) Sequence and architecture of DNA fragments used for immobilization; (Supplementary Figure S2) enrichment of stalled elongation complex (SEC); (Supplementary Figure S3A) Mt, Ec, and Ms RNAPs recognizing the T7A1 promoter; (Supplementary Figure S3B) termination of transcription by Rho; (Supplementary Figure S4) determination of transcription elongation rates for the template with GC-rich sequence (A−C); (Supplementary Figure S5) NTP injection in the presence and absence of EDTA (PDF)

Excel tables depicting the build-up of resonance units during transcription events at A+T-rich and G+C-rich templates; (Table S1) *E. coli* WT RNAP and A+T-rich template and distribution of RUs and calculated RU as a function of time; (Table S2) *E. coli* B8 RNAP and A+T-rich template and distribution of RUs and calculated RU as a function of time; (Table S3) distribution of $k1$ across transcription elongation complex species for *E. coli* WT and B8 RNAP; (Table S4) *M. smegmatis* RNAP and A+T-rich template and distribution of RUs and calculated RU as a function of time; (Table S5) *M. tuberculosis* RNAP and A+T-rich template and distribution of RUs and calculated RU as a function of time; (Table S6) distribution of $k1$ across transcription elongation complex species for *E. coli* WT, B8, *M. smegmatis*, and *M. tuberculosis* RNAP at the A+T-rich template; (Table S7) *M. smegmatis*, *M. tuberculosis* RNAP, and G+C-rich template and distribution of RUs and calculated RU as a function of time; (Table S8) distribution of $k1$ across transcription elongation complex species for *E. coli* WT, B8, *M. smegmatis*, and *M. tuberculosis* RNAP at the G+C template (XLSX)

Special Issue Paper

Published as part of *ACS Omega* virtual special issue "Nucleic Acids: A 70th Anniversary Celebration of DNA".

■ AUTHOR INFORMATION

Corresponding Author

Valakunja Nagaraja − *Department of Microbiology and Cell Biology, Indian Institute of Science, Bangalore 560012, India;* orcid.org/0000-0002-9768-1505; Phone: 91-80-2360 0668; Email: vraj@iisc.ac.in; Fax: +91-80-2360 2697

Authors

Priyanka Tare − *Department of Microbiology and Cell Biology, Indian Institute of Science, Bangalore 560012, India*

Tuhin Bhowmick − *Department of Physics, Indian Institute of Science, Bangalore 560012, India; Centre for Cellular and Molecular Platforms, NCBS-TIFR, Pandorum Technologies Pvt. Ltd., Bangalore 560065, India*

Gurunath Katagi − *Centre for Cellular and Molecular Platforms, NCBS-TIFR, Pandorum Technologies Pvt. Ltd., Bangalore 560065, India*

Arnab China − *Department of Microbiology and Cell Biology, Indian Institute of Science, Bangalore 560012, India*

Complete contact information is available at: https://pubs.acs.org/10.1021/acsomega.3c04754

Notes

The authors declare no competing financial interest.

■ ACKNOWLEDGMENTS

We thank Dr. Ranjan Sen (Centre for DNA Fingerprinting and Diagnostics, India) for providing the MG1655 B8 strain, M. S. Srilatha for SPR experiments, and V. N. Gauthami for technical assistance. The work is supported from grants from the Science and Engineering Research Board (CRG/2019/000077) and

Department of Biotechnology, Government of India (BT/PR13522/CoE/34/27/2015).

REFERENCES

(1) Hibbing, M. E.; Fuqua, C.; Parsek, M. R.; Peterson, S. B. Bacterial Competition: Surviving and Thriving in the Microbial Jungle. *Nat. Rev. Microbiol.* **2010**, *8*, 15.

(2) Palková, Z. Multicellular Microorganisms: Laboratory versus Nature. *EMBO Rep.* **2004**, *5* (5), 470−476.

(3) Nordholt, N.; van Heerden, J.; Kort, R.; Bruggeman, F. J. Effects of Growth Rate and Promoter Activity on Single-Cell Protein Expression. *Sci. Rep.* **2017**, *7* (1), 6299.

(4) Tolić-Nørrelykke, S. F.; Engh, A. M.; Landick, R.; Gelles, J. Diversity in the Rates of Transcript Elongation by Single RNA Polymerase Molecules. *J. Biol. Chem.* **2004**, *279* (5), 3292−3299.

(5) Yakhnin, A. v.; FitzGerald, P. C.; McIntosh, C.; Yakhnin, H.; Kireeva, M.; Turek-Herman, J.; Mandell, Z. F.; Kashlev, M.; Babitzke, P. NusG Controls Transcription Pausing and RNA Polymerase Translocation throughout the *Bacillus Subtilis* Genome. *Proc. Natl. Acad. Sci. U.S.A.* **2020**, *117* (35), 21628−21636.

(6) Harshey, R. M.; Ramakrishnan, T. Rate of Ribonucleic Acid Chain Growth in Mycobacterium Tuberculosis H37Rv. *J. Bacteriol.* **1977**, *129* (2), 616−622.

(7) Vogel, U.; Jensen, K. F. The RNA Chain Elongation Rate in *Escherichia coli* Depends on the Growth Rate. *J. Bacteriol.* **1994**, *176* (10), 2807−2813.

(8) Adelman, K.; La Porta, A.; Santangelo, T. J.; Lis, J. T.; Roberts, J. W.; Wang, M. D. Single Molecule Analysis of RNA Polymerase Elongation Reveals Uniform Kinetic Behaviour. *Proc. Natl. Acad. Sci. U.S.A.* **2002**, *99* (21), 13538−13543.

(9) Wang, M. D.; Schnitzer, M. J.; Yin, H.; Landick, R.; Gelles, J.; Block, S. M. Force and Velocity Measured for Single Molecules of RNA Polymerase. *Science* **1998**, *282* (5390), 902−907.

(10) Greive, S. J.; Weitzel, S. E.; Goodarzi, J. P.; Main, L. J.; Pasman, Z.; von Hippel, P. H. Monitoring RNA Transcription in Real Time by Using Surface Plasmon Resonance. *Proc. Natl. Acad. Sci. U.S.A.* **2008**, *105* (9), 3315−3320.

(11) Forde, N. R.; Izhaky, D.; Woodcock, G. R.; Wuite, G. J. L.; Bustamante, C. Using Mechanical Force to Probe the Mechanism of Pausing and Arrest during Continuous Elongation by *Escherichia coli* RNA Polymerase. *Proc. Natl. Acad. Sci. U.S.A.* **2002**, *99* (18), 11682−11687.

(12) Davenport, R. J.; Wuite, G. J.; Landick, R.; Bustamante, C. Single-Molecule Study of Transcriptional Pausing and Arrest by E. coli RNA Polymerase. *Science* **2000**, *287* (5462), 2497−2500.

(13) Yin, H.; Landick, R.; Gelles, J. Tethered Particle Motion Method for Studying Transcript Elongation by a Single RNA Polymerase Molecule. *Biophys. J.* **1994**, *67* (6), 2468−2478.

(14) Jin, D. J.; Gross, C. A. RpoB8, a Rifampicin-Resistant Termination-Proficient RNA Polymerase, Has an Increased Km for Purine Nucleotides during Transcription Elongation. *J. Biol. Chem.* **1991**, *266* (22), 14478−14485.

(15) Susa, M.; Sen, R.; Shimamoto, N. Generality of the Branched Pathway in Transcription Initiation by *Escherichia coli* RNA Polymerase. *J. Biol. Chem.* **2002**, *277* (18), 15407−15412.

(16) Sclavi, B.; Zaychikov, E.; Rogozina, A.; Walther, F.; Buckle, M.; Heumann, H. Real-Time Characterization of Intermediates in the Pathway to Open complex Formation by *Escherichia coli* RNA Polymerase at the T7A1 Promoter. *Proc. Natl. Acad. Sci. U.S.A.* **2005**, *102* (13), 4706−4711.

(17) China, A.; Mishra, S.; Tare, P.; Nagaraja, V. Inhibition of *Mycobacterium tuberculosis* RNA Polymerase by Binding of a Gre Factor Homolog to the Secondary Channel. *J. Bacteriol.* **2012**, *194* (5), 1009−1017.

(18) Kadesch, T. R.; Rosenberg, S.; Chamberlin, M. J. Binding of *Escherichia coli* RNA Polymerase Holoenzyme to Bacteriophage T7 DNA: Measurements of Binding at Bacteriophage T7 Promoter A1 Using a Template Competition Assay. *J. Mol. Biol.* **1982**, *155* (1), 1−29.

(19) Ahmad, E.; Mahapatra, V.; Vanishree, V. M.; Nagaraja, V. Intrinsic and Rho-Dependent Termination Cooperate for Efficient Transcription Termination at 3′ Untranslated Regions. *Biochem. Biophys. Res. Commun.* **2022**, *628*, 123−132.

(20) Ahmad, E.; Mitra, A.; Ahmed, W.; Mahapatra, V.; Hegde, S. R.; Sala, C.; Cole, S. T.; Nagaraja, V. Rho-Dependent Transcription Termination Is the Dominant Mechanism in *Mycobacterium tuberculosis*. *Biochim. Biophys. Acta, Gene Regul. Mech.* **2023**, *1866* (2), 194923.

(21) Rogozina, A.; Zaychikov, E.; Buckle, M.; Heumann, H.; Sclavi, B. DNA melting by RNA polymerase at the T7A1 promoter precedes the rate-limiting step at 37°C and results in the accumulation of an off-pathway intermediate. *Nucleic Acids Res.* **2009**, *37* (16), 5390−5404.

(22) Persson, B.; Stenhag, K.; Nilsson, P.; Larsson, A.; Uhlén, M.; Nygren, P. Analysis of Oligonucleotide Probe Affinities Using Surface Plasmon Resonance: A Means for Mutational Scanning. *Anal. Biochem.* **1997**, *246* (1), 34−44.

(23) Hoops, S.; Sahle, S.; Gauges, R.; Lee, C.; Pahle, J.; Simus, N.; Singhal, M.; Xu, L.; Mendes, P.; Kummer, U. COPASI—a complex PAthway SImulator. *Bioinformatics* **2006**, *22* (24), 3067−3074.

(24) Davidson, C. J.; Narang, A.; Surette, M. G. Integration of Transcriptional Inputs at Promoters of the Arabinose Catabolic Pathway. *BMC Syst. Biol.* **2010**, *4* (1), 75.

(25) Tare, P.; China, A.; Nagaraja, V.; Tyagi, A. K. Distinct and Contrasting Transcription Initiation Patterns at *Mycobacterium tuberculosis* Promoters. *PLoS One* **2012**, *7* (9), No. e43900.

(26) China, A.; Tare, P.; Nagaraja, V. Comparison of Promoter-Specific Events during Transcription Initiation in Mycobacteria. *Microbiology (N Y)* **2010**, *156* (7), 1942−1952.

(27) Mitra, A.; Misquitta, R.; Nagaraja, V.; Chatterji, D. *Mycobacterium tuberculosis* Rho Is an NTPase with Distinct Kinetic Properties and a Novel RNA-Binding Subdomain. *PLoS One* **2014**, *9* (9), No. e107474.

(28) Unniraman, S.; Prakash, R.; Nagaraja, V. Alternate Paradigm for Intrinsic Transcription Termination in Eubacteria. *J. Biol. Chem.* **2001**, *276* (45), 41850−41855.

(29) Kalyani, B. S.; Kunamneni, R.; Wal, M.; Ranjan, A.; Sen, R. A NusG Paralogue from *Mycobacterium tuberculosis*, Rv0639, Has Evolved to Interact with Ribosomal Protein S10 (Rv0700) but Not to Function as a Transcription Elongation−Termination Factor. *Microbiology* **2015**, *161* (1), 67−83.

(30) Shashni, R.; Mishra, S. S.; Sudha Kalayani, B.; Sen, R. Suppression of in Vivo Rho-Dependent Transcription Termination Defects: Evidence for Kinetically Controlled Steps. *Microbiology* **2012**, *158* (6), 1468−1481.

(31) Petushkov, I.; Pupov, D.; Bass, I.; Kulbachinskiy, A. Mutations in the CRE Pocket of Bacterial RNA Polymerase Affect Multiple Steps of Transcription. *Nucleic Acids Res.* **2015**, *43* (12), 5798−5809.

(32) Conrad, T. M.; Frazier, M.; Joyce, A. R.; Cho, B.-K.; Knight, E. M.; Lewis, N. E.; Landick, R.; Palsson, B. Ø. RNA Polymerase Mutants Found through Adaptive Evolution Reprogram *Escherichia coli* for Optimal Growth in Minimal Media. *Proc. Natl. Acad. Sci. U.S.A.* **2010**, *107* (47), 20500−20505.

(33) Lane, W. J.; Darst, S. A. Molecular Evolution of Multisubunit RNA polymerases: Sequence Analysis. *J. Mol. Biol.* **2010**, *395* (4), 671−685.

(34) Mejia, Y. X.; Nudler, E.; Bustamante, C. Trigger Loop Folding Determines Transcription Rate of *Escherichia coli's* RNA Polymerase. *Proc. Natl. Acad. Sci. U.S.A.* **2015**, *112* (3), 743−748.

(35) Iyer, L. M.; Aravind, L. Insights from the Architecture of the Bacterial Transcription Apparatus. *J.Struct. Biol.* **2012**, *179* (3), 299−319.

(36) Alifano, P.; Palumbo, C.; Pasanisi, D.; Talà, A. Rifampicin-Resistance, RpoB Polymorphism and RNA Polymerase Genetic Engineering. *J. Biotechnol.* **2015**, *202*, 60−77.

(37) Wee, L. M.; Tong, A. B.; Florez Ariza, A. J.; Cañari-Chumpitaz, C.; Grob, P.; Nogales, E.; Bustamante, C. J. A Trailing Ribosome

https://doi.org/10.1021/acsomega.3c04754
ACS Omega 2023, 8, 47510−47519

Speeds up RNA Polymerase at the Expense of Transcript Fidelity via Force and Allostery. *Cell* **2023**, *186* (6), 1244−1262.e34.
(38) Niederweis, M. Nutrient Acquisition by Mycobacteria. *Microbiology* **2008**, *154* (3), 679−692.
(39) Cox, R. A. Quantitative Relationships for Specific Growth Rates and Macromolecular Compositions of *Mycobacterium tuberculosis*, *Streptomyces coelicolor A3(2)* and *Escherichia coli* B/r: An Integrative Theoretical Approach. *Microbiology* **2004**, *150* (5), 1413−1426.
(40) Cox, R. A. Correlation of the rate of protein synthesis and the third power of the RNA : protein ratio in Escherichia coli and Mycobacterium tuberculosis. *Microbiology* **2003**, *149* (3), 729−737.
(41) Kenri, T.; Imamoto, F.; Kano, Y. Three Tandemly Repeated Structural Genes Encoding tRNAf1Met in the *MetZ* Operon of *Escherichia coli* K-12. *Gene* **1994**, *138* (1−2), 261−262.
(42) Dastur, A.; Kumar, P.; Ramesh, S.; Vasanthakrishna, M.; Varshney, U. Analysis of the Initiator *tRNA* Genes from a Slow- and a Fast-Growing Mycobacterium. *Arch. Microbiol.* **2002**, *178* (4), 288−296.
(43) Gonzalez-y-Merchand, J. A.; Garcia, M. J.; Gonzalez-Rico, S.; Colston, M. J.; Cox, R. A. Strategies Used by Pathogenic and Nonpathogenic Mycobacteria to Synthesize rRNA. *J. Bacteriol.* **1997**, *179* (22), 6949−6958.
(44) Gonzalez-y-Merchand, J. A.; Colston, M. J.; Cox, R. A. The rRNA Operons of *Mycobacterium smegmatis* and *Mycobacterium tuberculosis*: Comparison of Promoter Elements and of Neighbouring Upstream Genes. *Microbiology* **1996**, *142* (3), 667−674.
(45) Schneider, D. A.; Gourse, R. L. Changes in *Escherichia coli* rRNA Promoter Activity Correlate with Changes in Initiating Nucleoside Triphosphate and Guanosine 5′ Diphosphate 3′-Diphosphate Concentrations after Induction of Feedback Control of Ribosome Synthesis. *J. Bacteriol.* **2003**, *185* (20), 6185−6191.
(46) Miller, O. L.; Hamkalo, B. A.; Thomas, C. A. Visualization of Bacterial Genes in Action. *Science* **1970**, *169* (3943), 392−395.
(47) Jha, R. K.; Tare, P.; Nagaraja, V. Regulation of the *Gyr* Operon of *Mycobacterium tuberculosis* by Overlapping Promoters, DNA Topology, and Reiterative Transcription. *Biochem. Biophys. Res. Commun.* **2018**, *501* (4), 877−884.
(48) China, A.; Nagaraja, V. Purification of RNA polymerase from mycobacteria for optimized promoter-polymerase interactions. *Protein Expression Purif.* **2010**, *69* (2), 235−242.

https://doi.org/10.1021/acsomega.3c04754
ACS Omega 2023, 8, 47510−47519